Diffusion of a ring polymer in good solution via the Brownian dynamics with no bond crossing

2008 J. Phys. A: Math. Theor. 41 145004

(http://iopscience.iop.org/1751-8121/41/14/145004)

IOP PUBLISHING JOURNAL OF PHYSICS A: MATHEMATICAL AND THEORETICAL

J. Phys. A: Math. Theor. **41** (2008) 145004 (11pp) doi:10.1088/1751-8113/41/14/145004

Diffusion of a ring polymer in good solution via the Brownian dynamics with no bond crossing

Naoko Kanaeda and Tetsuo Deguchi

Department of Physics, Ochanomizu University, Tokyo 112-8610, Japan

E-mail: kanaeda@degway.phys.ocha.ac.jp and deguchi@phys.ocha.ac.jp

Received 4 December 2007, in final form 28 February 2008
Published 26 March 2008
Online at stacks.iop.org/JPhysA/41/145004

Abstract

Diffusion constants D_R and D_L of ring and linear polymers of the same molecular weight in a good solvent, respectively, have been evaluated through the Brownian dynamics with hydrodynamic interaction in which no bond crossing is possible. The ratio $C = D_R/D_L$, which should be universal in the context of the renormalization group, has been estimated as $C = 1.14 \pm 0.01$ for the large-N limit. It should be consistent with that of synthetic polymers, while it is smaller than that of DNAs such as $C \approx 1.3$. We also perform the same simulation through Brownian dynamics with hydrodynamic interaction where bond crossings are possible, and obtain almost the same estimate for the ratio C.

PACS numbers: 83.10.Mj, 83.10.Rs, 82.35.Lr, 66.10.Cb, 87.14.Gg, 02.10.Kn

1. Introduction

Recently, there has been much progress in experimental techniques associated with ring polymers. Ring polymers of large molecular weights are synthesized not only quite effectively [1] but also with small dispersions and high purity [2, 3]. Diffusion constants of linear, relaxed circular and supercoiled DNAs have been measured quite accurately [4]. Furthermore, hydrodynamic radius of circular DNA has also been measured [5]. The developments are quite remarkable. In fact, it used to be considered quite difficult to synthesize ring polymers of large molecular weights. It has now become quite interesting to evaluate numerically dynamical or conformational quantities of linear and ring polymers that can be measured in experiments.

It should be nontrivial how linear and ring polymers with the same molecular weight in solution may have different dynamical or conformational properties. In fact, the excluded volume effect should play a more significant role for ring polymers than for linear polymers, since the average distance among monomers is smaller due to the constraint of closing two ends [6]. Moreover, in a dilute solution, the topology of a given ring polymer is conserved

under thermal fluctuations [7] and represented by a knot. Topological constraints may lead to nontrivial statistical mechanical or dynamical properties of ring polymers [8–17].

In this paper we discuss diffusion constants D_R and D_L of ring and linear polymers in good solution, respectively, via the Brownian dynamics with hydrodynamic interaction in which bond crossings are effectively prohibited. Here the ring and linear polymers have the same molecular weight, and we calculate diffusion constants for several different values of the number of segments, N, for $5 < N < 50$. We then calculate the ratio $C = D_R/D_L$ and compare it with the values measured in some experiments and other theoretical values. This gives a test for the validity of dynamical models of ring and linear polymers. In fact, it is suggested from the renormalization group argument that the large-N limit of C should be universal among some class of polymer models. Hereafter we call the Brownian dynamics with no bond crossings *dynamics A*.

Furthermore, we also perform the Brownian dynamics with hydrodynamic interaction under almost the same molecular potentials as dynamics A except the parameters of the finite extensible nonlinear elongational (FENE) potential which determine the maximal distance between neighboring monomers. We set the maximal distance larger so that bond crossings are allowed. We call it *dynamics B*. Dynamics B has precisely the same potential parameters as that of [18]. We have found that bond crossings occurred for dynamics B, checking the topology of the ring polymer by calculating some knot invariants at every time step of the Brownian dynamics.

Simulation results of both dynamics A and B should be important. In fact, there have been several simulation results obtained and accumulated for dynamics B [18, 19]. We may compare the present simulation with previous ones. In this sense, dynamics B is a standard algorithm in the Brownian dynamics. Furthermore, dynamics A is important since it preserves the initial topology of a ring polymer.

The present study should be useful for making explicit connections between experimental and theoretical results of dilute solutions of ring polymers. In fact, for dilute ring-polymer solutions, even some fundamental properties such as the effects of topological constraints have not been clearly confirmed in experiments, yet. Through simulations, we can study the effects of topological constraints, which can be checked in experiments.

The content of the paper consists of the following. In section 2, we briefly explain the simulation method. In section 3, we discuss two simulation results. In section 3.1, the ratio of the mean-square radii of gyration of ring and linear polymers, g, are evaluated numerically. The value of g for dynamics B is consistent with the lattice simulation result, while that of dynamics A is larger than the standard one. We confirm it also by the Monte Carlo simulation. It should thus be an interesting future problem to evaluate the ratio g for larger values of N. In section 3.2, we discuss the ratio C both for dynamics A and B. We find that the estimates of C are given by almost the same value both for dynamics A and B. Interestingly, the estimate of C is consistent with a theoretical value given by a perturbation theory, while it is different from that of the renormalization group calculation in one-loop order. However, we should note that a one-loop order evaluation could give only a rough estimate and multi-loop corrections could improve it.

2. Simulation method

The ring-polymer molecule is modeled as a cyclic bead-and-spring chain with N beads connected by N FENE springs with the following force law:

$$\boldsymbol{F}(\boldsymbol{r}) = -H\boldsymbol{r}\big/\big(1 - r^2\big/r_{\max}^2\big), \tag{1}$$

where $r = |\boldsymbol{r}|$. Let us denote by b the unit of distance. Here we assume that the average distance between neighboring monomers is approximately given by b. We set constants H and $r_{\max}$ as follows: $H = 30k_BT/b^2$ and $r_{\max} = 1.3b$ for dynamics A, and $H = 3k_BT/b^2$ and $r_{\max} = 10b$ for dynamics B. We assume the Lennard–Jones (LJ) potential acting among monomers as follows:

$$V(r) = 4\epsilon_{\mathrm{LJ}}\left[\left(\frac{\sigma_{\mathrm{LJ}}}{r_{ij}}\right)^{12} - \left(\frac{\sigma_{\mathrm{LJ}}}{r_{ij}}\right)^{6}\right]. \tag{2}$$

Here r_{ij} is the distance of beads i and j, and ϵ_{LJ} and σ_{LJ} denote the minimum energy and the zero-energy distance, respectively [19]. We set the Lennard–Jones parameters as $\sigma_{\mathrm{LJ}} = 0.8b$ and $\epsilon_{\mathrm{LJ}} = 0.1k_BT$ so that they give good solvent conditions [18]. Here k_B denotes the Boltzmann constant.

We employ the predictor–corrector version [20] of the Ermak–McCammon algorithm [21] for generating the time evolution of a ring polymer in solution. The details are given in appendix A. The hydrodynamic interaction is taken into account through the Ronte–Prager–Yamakawa tensor [22, 23] where the bead friction is given by $\zeta = 6\pi\eta_s a$ with the bead radius $a = 0.257b$ and a dimensionless hydrodynamic interaction parameter $h^* = (\zeta/6\pi\eta_s)\sqrt{H/\pi k_BT} = 0.25$.

In the present simulation, physical quantities are given in dimensionless units such as in [19]. We divide length by b, energy by k_BT and time by $\zeta b^2/k_BT$. Let us indicate dimensionless quantities by an asterisk as superscript. We have $H^* = 30, r^*_{\max} = 1.3$ for dynamics A, and $H^* = 3, r^*_{\max} = 10$ for dynamics B. We take the simulation time step $\Delta t^* = 10^{-4}$.

When we evaluate the mean-square radius of gyration and the diffusion constant for ring and linear polymers through the Brownian dynamics with hydrodynamic interaction, we keep each run long enough so that the diffusion constant approaches its equilibrium value. For instance, in the case of linear polymers of $N = 45$ of dynamics A, we have performed 9.4×10^5 time steps for each run. After the average value of the diffusion constant approaches some equilibrium value, we start sampling the data and pick up one conformation out of every 18 800 time steps. Then, the diffusion constant evaluated at 740 000th time step is given by 9.256×10^{-2}, while that at 940 000th time step is given by 9.276×10^{-2}. The difference 0.020×10^{-2} is smaller than their probable error 0.068×10^{-2}.

3. Simulation results

3.1. Ratio of the mean-square radii of gyration

The mean-square radius of gyration $\langle R_G^2 \rangle$ of a polymer consisting of N monomers is defined by

$$\langle R_G^2 \rangle = \frac{1}{N}\sum_{j=1}^{N}\langle(\vec{r}_j - \vec{r}_G)^2\rangle$$

where $\vec{r}_j$ denote the position vectors of monomers for $j = 1, 2, \ldots, N$ and $\vec{r}_G$ is the position vector of the center of mass of the polymer. The symbol $\langle A \rangle$ denotes the ensemble average of physical quantity A.

Let us discuss the estimates of the mean-square radius of gyration for ring and linear polymers, $\langle R_G^2 \rangle_R$ and $\langle R_G^2 \rangle_L$, respectively, obtained by dynamics A and B. They are plotted in figure 1 against the number of segments N in the double logarithmic scales and are given in table 1. It is clear that they are fitted well by straight lines. It seems that the N-dependence is close to that of the asymptotic behavior, although the number of segments N are not very

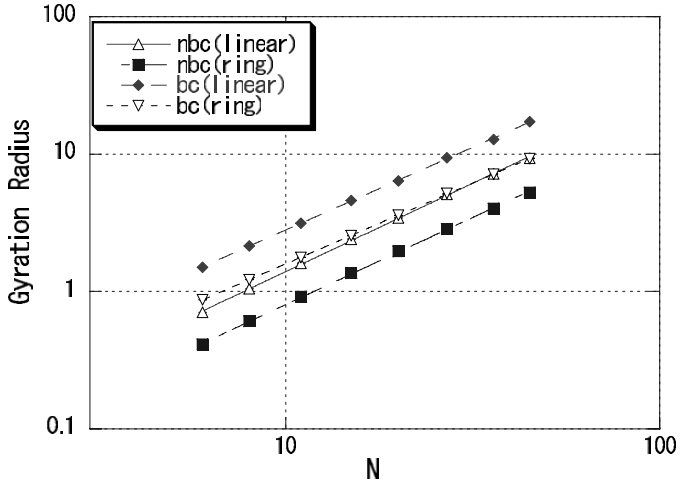

Figure 1. Mean-square radius of gyration $\langle R_G^2\rangle_L$ and $\langle R_G^2\rangle_R$ for dynamics A (no bond crossing, nbc) and B (allowed bond crossings, bc). For dynamics A, data points of linear polymers are shown by (△), where ring polymers by (■), where $A_R = 0.043 \pm 0.0001$ and $\nu_R = 1.270 \pm 0.001$. For dynamics B, linear polymers by (♦), where $A_L = 0.175 \pm 0.001$ and $\nu_L = 1.204 \pm 0.002$; ring polymers by (▽), where $A_R = 0.105 \pm 0.001$ and $\nu_R = 1.179 \pm 0.001$.

Table 1. Dynamics A (no bond crossing): mean-square radii of gyration for linear and ring polymers, $\langle R_G^2\rangle_R$ and $\langle R_G^2\rangle_L$, and the g values. Applying the least-square method for $\langle R_G^2\rangle_L = A_L N^{2\nu_L}$ and $\langle R_G^2\rangle_R = A_R N^{2\nu_R}$, respectively, the following estimates are obtained: $2\nu_L = 1.288 \pm 0.002$, $A_L = 0.072 \pm 0.001$; $2\nu_R = 1.270 \pm 0.001$, $A_R = 0.043 \pm 0.001$. In all the tables, errors are given by probable errors.

N	$\langle R_G^2\rangle_R$	$\langle R_G^2\rangle_L$	$g = \langle R_G^2\rangle_R / \langle R_G^2\rangle_L$
6	0.413 ± 0.001	0.705 ± 0.003	0.586 ± 0.003
8	0.606 ± 0.001	1.046 ± 0.004	0.579 ± 0.003
11	0.916 ± 0.002	1.605 ± 0.007	0.571 ± 0.004
15	1.364 ± 0.002	2.404 ± 0.012	0.567 ± 0.004
20	1.961 ± 0.005	3.431 ± 0.018	0.571 ± 0.004
27	2.842 ± 0.008	5.082 ± 0.024	0.559 ± 0.004
36	4.028 ± 0.011	7.182 ± 0.037	0.561 ± 0.004
45	5.260 ± 0.016	9.335 ± 0.053	0.563 ± 0.005

large, yet. As we shall discuss later, it is probably due to the effect of the off-lattice molecular potentials employed in the dynamics. Thus, as a fitting formula, we employ the large-N asymptotic behavior of the mean-square radius of gyration, $\langle R_G^2\rangle = AN^{2\nu}$. The estimates of the fitting parameters, A_R and ν_R for ring polymers, and A_L and ν_L for linear polymers, are given in the caption of figure 1.

Let us now define the geometric shrinking factor g by [24]

$$g = \langle R_G^2\rangle_R / \langle R_G^2\rangle_L. \tag{3}$$

We assume that exponent ν should be the same for ring and linear chains, i.e. $\nu_R = \nu_L$. We thus have the following fitting formula with three parameters:

$$g = g_\infty(1 + B_g N^{-\Delta_g}). \tag{4}$$

Applying (4), we have $g_\infty = 0.559 \pm 0.007$ for dynamics A and $g_\infty = 0.535 \pm 0.002$ for dynamics B, as shown in figure 2.

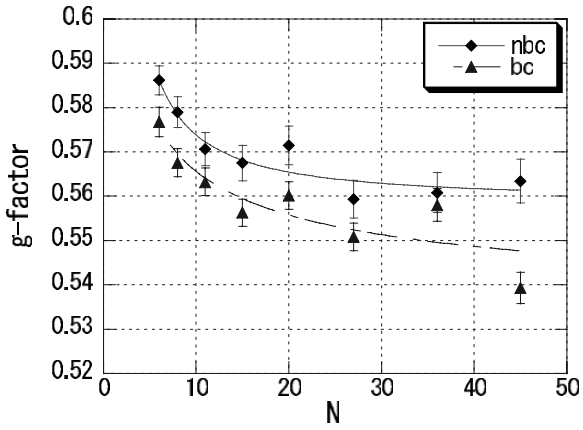

Figure 2. The ratio $g = \langle R_G^2 \rangle_R / \langle R_G^2 \rangle_L$ versus N with the fitting curve (4). For dynamics A shown by (♦) (nbc), we have $g_\infty = 0.559 \pm 0.007$, $B_g = 0.402 \pm 0.438$ and $\Delta_g = 1.173 \pm 0.706$. Here $\chi^2 = 3.3$ for eight data points. For dynamics B shown by (▲) (bc), we have $g_\infty = 0.535 \pm 0.002 B_g = 0.204 \pm 0.079$ and $\Delta_g = 0.565 \pm 0.476$. Here $\chi^2 = 14.9$ for eight data points.

The estimate of g value for dynamics B, $g_\infty = 0.535 \pm 0.002$, should be consistent with the Monte Carlo simulation using the bond fluctuation model [25]. Interestingly, however, the estimate of g_∞ for dynamics A is larger than that of dynamics B even if we take into account their errors. The enhancement of value g_∞ in dynamics A should be due to the potential forces. In fact, we have confirmed that almost the same value of g_∞ is obtained by the Monte Carlo simulation with the same molecular potentials as dynamics A. Therefore, we conclude that it is due to the potential forces employed in dynamics A. Here, the potential function of the Monte Carlo simulation of linear chains is given by the following:

$$-\sum_{i=1}^{N-1} 0.5 H r_{\max}^2 \ln[1 - (r_{i,i+1}/r_{\max})^2] + 4\epsilon_{\mathrm{LJ}} \sum_{i>j}^{N} [(\sigma_{\mathrm{LJ}}/r_{ij})^{12} - (\sigma_{\mathrm{LJ}}/r_{ij})^6].$$

For ring chains, we add a term of $r_{N,1}$ due to the periodicity.

Here we note that we have employed the symbol g_∞ for the fitting parameter, expecting that it should suggest the asymptotic value of g. However, in order to evaluate the true asymptotic value of g, we have to perform simulations for larger values of N. It should thus be an interesting future problem whether the enhancement of value g should be relevant to the asymptotic value of g or not.

According to the one-loop renormalization group calculation [26] g is given by

$$g_\infty = \exp(13/96)/2 = 0.573. \tag{5}$$

The value (5) is larger than the estimates, $g_\infty = 0.559 \pm 0.007$ for dynamics A and $g_\infty = 0.535 \pm 0.002$ for dynamics B. Thus, the one-loop calculation does not explain the estimate of g_∞ for dynamics A or B. However, we should note that it is possible that the one-loop RG result gives only a crude approximation, and higher-order calculation improves the g value. Here we note that for the ϵ-expansion of the n-vector model, higher-order terms have been calculated in order to evaluate universal quantities [27]. Thus, the multi-loop corrections should be important, although the one-loop correction [26] is based on Fixman's cluster expansion [28] and it is not clear whether one can extend it.

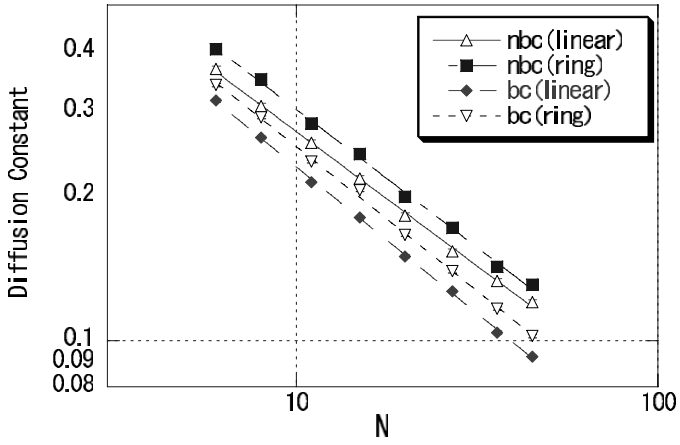

Figure 3. Diffusion constants of ring and linear polymers for dynamics A (nbc) depicted by (△) and (■), respectively, for dynamics B (bc) (♦) and (▽), respectively. The horizontal axis denotes the number of segments, N.

Through perturbation calculation, g was estimated in terms of the excluded-volume parameter z as follows [29, 30]:

$$g = \frac{1}{2}\left[1 + \left(\frac{\pi}{2} - \frac{134}{105}\right) z + \cdots\right]. \tag{6}$$

The value of g is dependent on the excluded-volume parameter, z. In order to have $g \approx 0.53$, we have $z \approx 0.20$. Here we note that the value z depends on the number of segments N. In order to have $z \approx 0.20$ we have to adjust many model parameters. Thus, it should be practically impossible to give good estimates of g by making use of the perturbation theory.

3.2. Ratio of diffusion constants

Let us recall that the diffusion constant of a polymer is defined by the following:

$$D = \lim_{t\to\infty} \frac{1}{6t} \langle (\vec{r}_G(t) - \vec{r}_G(0))^2 \rangle. \tag{7}$$

Here $\vec{r}_G(t)$ denote the position vector of the center of mass of the polymer. Making use of (7) we have evaluated the diffusion constant of ring and linear polymers, D_R and D_L, respectively, through dynamics A and B.

According to the Einstein relation, the diffusion constant of a polymer should be given by $D = k_B T/\zeta$ where ζ is given by $\zeta = 6\pi\eta R_H$ with viscosity η and the hydrodynamic radius R_H. Let us assume that the hydrodynamic radius R_H has the same asymptotic scaling behavior with the square root of the mean-square radius of gyration, $\sqrt{\langle R_G^2 \rangle} \propto N^{\nu}$. Thus, in a dilute solution, we have the following large-N behavior:

$$D = \frac{k_B T}{6\pi\eta R_H} \propto N^{-\nu}. \tag{8}$$

Taking the analogy of the large-N behavior (8), we introduce the following fitting formulae: $D_R = A(D_R) N^{-\nu(D_R)}$ and $D_L = A(D_L) N^{-\nu(D_L)}$. Applying them to the data of table 2, we have the estimates as shown in the caption of figure 3. The fitting curves are shown in figure 3. The estimates of $\nu(D_R)$ and $\nu(D_L)$ are consistent with the expected N-dependence: $D_R, D_L \propto N^{-\nu}$ with $\nu \approx 0.59$.

Table 2. Dynamics B (allowed bond crossings): mean-square radii of gyration for linear and ring polymers, $\langle R_G^2\rangle_R$ and $\langle R_G^2\rangle_L$, and the g values. Applying the least-square method for $\langle R_G^2\rangle_L = A_L N^{2\nu_L}$ and $\langle R_G^2\rangle_R = A_R N^{2\nu_R}$, respectively, the following estimates are obtained: $2\nu_L = 1.204 \pm 0.002$, $A_L = 0.175 \pm 0.001$; $2\nu_R = 1.179 \pm 0.001$, $A_R = 0.105 \pm 0.001$.

N	$\langle R_G^2\rangle_R$	$\langle R_G^2\rangle_L$	$g = \langle R_G^2\rangle_R / \langle R_G^2\rangle_L$
6	0.868 ± 0.002	1.505 ± 0.005	0.577 ± 0.003
8	1.221 ± 0.003	2.151 ± 0.008	0.568 ± 0.003
11	1.774 ± 0.004	3.149 ± 0.011	0.563 ± 0.003
15	2.550 ± 0.005	4.583 ± 0.016	0.556 ± 0.003
20	3.587 ± 0.008	6.404 ± 0.022	0.560 ± 0.003
27	5.172 ± 0.012	9.389 ± 0.037	0.551 ± 0.003
36	7.155 ± 0.017	12.821 ± 0.054	0.558 ± 0.004
45	9.306 ± 0.023	17.264 ± 0.070	0.539 ± 0.004

Table 3. Dynamics A (no bond crossing): diffusion constants of ring and linear polymers, D_R and D_L, and the C values. Each estimate is derived from the average over more than 2000 runs. We have $A(D_R) = 1.011 \pm 0.012$, $\nu(D_R) = 0.601 \pm 0.004$; $A(D_L) = 0.938 \pm 0.107$, $\nu(D_L) = 0.610 \pm 0.004$.

N	D_R	D_L	$C = D_R/D_L$
6	0.404 ± 0.005	0.368 ± 0.005	1.099 ± 0.028
8	0.350 ± 0.004	0.308 ± 0.004	1.137 ± 0.029
11	0.284 ± 0.004	0.258 ± 0.003	1.098 ± 0.028
15	0.244 ± 0.003	0.218 ± 0.003	1.123 ± 0.028
20	0.199 ± 0.003	0.182 ± 0.002	1.095 ± 0.027
27	0.172 ± 0.002	0.152 ± 0.002	1.120 ± 0.028
36	0.142 ± 0.002	0.133 ± 0.002	1.071 ± 0.024
45	0.131 ± 0.002	0.120 ± 0.001	1.087 ± 0.026

Table 4. Dynamics B (allowed bond crossings): diffusion constants of ring and linear polymers, D_R and D_L, and the C values. Each estimate is given by the average over more than 4000 runs. We have $A(D_R) = 1.138 \pm 0.022$, $\nu(D_R) = 0.575 \pm 0.007$; $A(D_L) = 1.138 \pm 0.022$, $\nu(D_L) = 0.610 \pm 0.004$.

N	D_R	D_L	$C = D_R/D_L$
6	0.341 ± 0.003	0.316 ± 0.002	1.078 ± 0.016
8	0.292 ± 0.002	0.265 ± 0.002	1.102 ± 0.016
11	0.236 ± 0.002	0.214 ± 0.002	1.104 ± 0.016
15	0.206 ± 0.001	0.180 ± 0.001	1.140 ± 0.016
20	0.166 ± 0.001	0.150 ± 0.001	1.109 ± 0.016
27	0.139 ± 0.001	0.127 ± 0.001	1.100 ± 0.017
36	0.117 ± 0.001	0.104 ± 0.001	1.122 ± 0.018
45	0.102 ± 0.001	0.093 ± 0.001	1.107 ± 0.017

Thus, formula (8) gives good fitting curves to the graphs of the diffusion constants D_R and D_L versus N, and the estimates of the exponents $\nu(D_R)$ and $\nu(D_L)$ are at least roughly in agreement with the SAW exponent $\nu_{\mathrm{SAW}} = 0.588$, although the large-$N$ behavior (8) should be valid only when N is asymptotically large enough. It is likely that $N = 50$ is not large enough to investigate any asymptotic behavior of the diffusion constants.

It is clear from tables 3 and 4 that the estimates of C are almost the same for dynamics A and B. Here, in figure 4, the C values are plotted against the number of segments N for

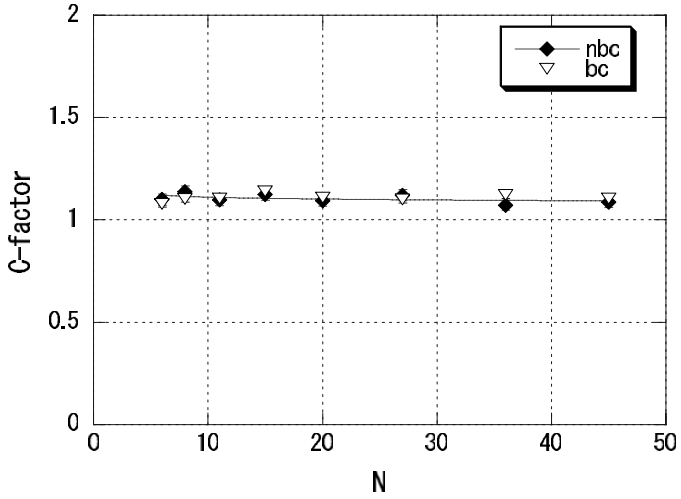

Figure 4. Ratio $C = D_R/D_L$ versus N. For dynamics A (♦) with fitting curve (9), $C_\infty = 1.14 \pm 0.01$, $B_C = 0.094 \pm 76.4$ and $\Delta_C = 2.98 \pm 454.97$. Here $\chi^2 = 6.0$ for eight data points. For dynamics B (▽), $C_\infty = 1.11 \pm 0.01$, $B_C = 161.8 \pm 2010.3$ and $\Delta_C = 4.78 \pm 6.94$. Here $\chi^2 = 5$ for eight data points.

dynamics A and B, respectively. We also observe that the estimates of C are independent of the number of segments, N. In fact, it is also the case with the experimental results of DNAs [4].

Let us assume again that exponent ν should be the same for the diffusion constants of ring and linear chains, D_R and D_L, respectively. Applying the fitting formula

$$C = C_\infty(1 + B_C N^{-\Delta_C}), \tag{9}$$

we obtain the following estimate: $C_\infty = 1.14 \pm 0.01$ for dynamics A; $C_\infty = 1.11 \pm 0.01$ for dynamics B. The fitting curves are shown in figure 4.

According to the one-loop renormalization group calculation in the presence of both hydrodynamic and self-avoiding interactions [31, 32], a universal ratio C is given by

$$C_\infty \equiv \lim_{N\to\infty} D_R/D_L = \exp(3/8) = 1.454. \tag{10}$$

The value (10) is much larger than the estimate of $C = 1.14 \pm 0.01$ for dynamics A and $C = 1.11 \pm 0.01$ for dynamics B. As in the case of the g value, it is possible that the one-loop order result gives only a crude result. Thus, higher-order RG corrections should be important. Here we note that the one-loop calculation was performed through the conformation-space renormalization-group approach [28], and it would be nontrivial to calculate higher-order corrections.

In recent years, the ratio C has been estimated by the perturbative calculation in terms of the excluded-volume parameter z [33],

$$C = D_R/D_L = \frac{3\pi}{8}\left(\frac{1 + 1.827z}{1 + 1.890z}\right)^{1/3}. \tag{11}$$

The value of C is rather constant with respect to z. We have 1.178 at $z = 0$, and 1.165 at $z = \infty$. It is interesting to note that the theoretical value (11) is rather close to the simulation value, $C = 1.14 \pm 0.01$. Thus, the perturbative calculation gives a theoretical value consistent with the simulation result although the validity of the perturbation theory is not clear.

Diffusion constants D_R and D_L have been measured in several experiments. We observe a tendency that for synthetic polymers C is given by 1.1–1.2, while for linear and circular DNAs it is roughly given by 1.3. For instance, it is estimated for relaxed circular DNAs as $C = 1.32 \pm 0.014$ [4]. For synthetic polymers through scattering experiments, $C = 1.1$–1.2 [34] and $C = 1.07$–1.15 [35]. Here we note that in [36] C is estimated as a little larger value than in other synthetic polymer experiments.

We thus conclude that the present model of ring and linear polymers should be valid for synthetic polymers, while for relaxed circular DNAs some additional potential energy might be important.

4. Conclusion

In the present model of the Brownian dynamics both for dynamics A and B, the estimate of $C = D_R/D_L$ should be consistent with that of synthetic polymer experiments, while it is smaller than that of DNA experiments. The difference in the ratio C between synthetic polymers and DNAs may be due to some additional potential functions arising from the closed DNA double strands.

Acknowledgments

The authors would like to thank Dr K Tsurusaki for helpful discussions and valuable comments. They are also grateful to Mirei Takasoe for useful comments. The present study is partially supported by Grant-in-Aid for Scientific Research Tokutei Ryouiki 19031007.

Appendix A. Algorithm of the Brownian dynamics

In this paper, we have simulated linear and ring polymers in a good solvent with hydrodynamic interaction by the revised version of the Brownian dynamics [21] with respect to the first-order predictor–corrector [20].

Let us explain the original version of the Brownian dynamics [21]. We consider N Brownian particles in a solvent of temperature T with hydrodynamic interaction. The position of the ith Brownian particle, $\vec{r}_i$, at time $t + \Delta t$ is calculated by the following equation:

$$\Delta\vec{r}_i = \vec{r}_i(t + \Delta t) - \vec{r}_i(t) = \sum_j \frac{\partial D_{ij}}{\partial \vec{r}_j} + \sum_j \frac{D_{ij}\vec{F}_j}{k_B T} + \vec{R}_i(\Delta t), \tag{A.1}$$

for $i, j = 1, 2, \ldots, N$. Here, D_{ij} denote the diffusion tensor, $\vec{F}_j$ the force acting on the jth particle, which we shall specify shortly. $\vec{R}_i(\Delta t)$ denote random numbers obeying the Gaussian distribution with $\langle \vec{R}_i(\Delta t)\rangle = 0$ and $\langle R_{i\alpha}(\Delta t) R_{j\beta}(\Delta t)\rangle = 2D_{ij}\delta_{\alpha\beta}\Delta t$.

We derive (A.1) as follows. First, we consider the Fokker–Planck equation of N Brownian particles in a solvent

$$\frac{\mathrm{d}W}{\mathrm{d}t} = \sum_i \sum_j \left(\frac{\partial}{\partial \vec{r}_i} D_{ij} \frac{\partial W}{\partial \vec{r}_j} - \frac{1}{kT} \vec{F}_j W \right), \tag{A.2}$$

where $W = W(\vec{r}_1, \ldots, \vec{r}_N, t)$ is the distribution function for the configuration space of the N particles. We can show that the distribution function is given by the multi-variable Gaussian distribution if the initial configuration of the N Brownian particles is given by

$W(\vec{r}_1^0, \ldots, \vec{r}_N^0, 0) = \prod_i \delta(\vec{r}_i - \vec{r}_i^0)$. Up to the first order of Δt, the average value and the variance–covariance of the Gaussian distribution, respectively, are given by the following:

$$\langle \Delta \vec{r}_i \rangle = \sum_j \frac{\partial}{\partial \vec{r}_i} D_{ij} \left(\frac{\partial W}{\partial \vec{r}_j} - \frac{1}{kT} \vec{F}_j W \right), \tag{A.3}$$

$$\langle \Delta r_{i\alpha} \Delta r_{j\beta} \rangle = 2 D_{ij} \delta_{\alpha\beta} \Delta t. \tag{A.4}$$

We thus obtain equation (A.1) from the conditions that the difference of the position vector $\Delta \vec{r}_i = \vec{r}_i(t + \Delta t) - \vec{r}_i(t)$ should satisfy the average value (A.3) and the variance–covariance (A.4). Here we remark that we can obtain the same average value (A.3) and the variance–covariance (A.4) by integrating the Langevin equations of N Brownian particles.

Let us now formulate the diffusion tensor and the force acting on the Brownian particles. We employ the Ronte–Prager–Yamakawa tensor as the diffusion tensor [22, 23],

$$D_{ij} = \frac{kT}{6\pi\zeta a} \delta_{ij} \qquad (\text{for } i = j) \tag{A.5}$$

$$D_{ij} = \frac{kT}{8\pi\zeta r_{ij}} \left[\left(E + \frac{\vec{r}_{ij}\vec{r}_{ij}}{r_{ij}^2} \right) + \frac{2a^2}{r_{ij}^2} \left(\frac{1}{3} E - \frac{\vec{r}_{ij}\vec{r}_{ij}}{r_{ij}^2} \right) \right] \qquad (\text{for } i \neq j). \tag{A.6}$$

Here a denotes the radius of a bead and ζ the hydrodynamic friction. For the force, we assume the Lennard–Jones force and the FENE spring force. The Lennard–Jones potential is given by

$$V_{\mathrm{LJ}} = 4\epsilon_{\mathrm{LJ}} \left(\left(\frac{\sigma_{\mathrm{LJ}}}{r} \right)^{12} - \left(\frac{\sigma_{\mathrm{LJ}}}{r} \right)^{6} \right), \tag{A.7}$$

where r is the distance between two particles, σ_{LJ} is the zero-energy distance and ϵ_{LJ} is the energy at distance σ. We give $\sigma_{\mathrm{LJ}} = 0.8b$ and $\epsilon_{\mathrm{LJ}} = 0.1 k_B T$ for simulation in a good solvent. The potential of the FENE spring force is given by

$$V_{\mathrm{FENE}} = -\frac{1}{2} r_{\max}^2 H \ln \left[1 - \left(\frac{r}{r_{\max}} \right)^2 \right], \tag{A.8}$$

where r is the distance between a pair of neighboring particles, H is the spring constant and $r_{\max}$ is the maximal distance between neighboring particles. For dynamics B, we set $H^* = 3.0$ and $r_{\max}^* = 10.0$, which are given in [19]. For dynamics A, we set $H^* = 30.0$ and $r_{\max}^* = 1.3$, as shown in [37]. In this model, no bond crossing should be possible due to the strong spring constant and the small maximal distance between neighboring particles. Here we note that dimensionless parameters and variables are obtained by dividing length, time and energy by b, $\zeta b^2/kT$ and kT, respectively.

The first-order predictor–corrector version [20] of the Ermak and McCammon algorithm [21] is given as follows. When initial positions of all particles $\vec{r}_i^0$ are given, we calculate the positions at the next time step as follows. First, we calculate the diffusion tensor and the force, i.e. D_{ij}^0 and $\vec{F}_i^0$, respectively, making use of (A.6)–(A.8). Second, we calculate the positions of all particles, $\vec{r}_i'$, by (A.1) with respect to D_{ij}^0 and $\vec{F}_i^0$. Third, using $\vec{r}_i'$, we again calculate the diffusion tensor and the force, and denote them by D_{ij}' and $\vec{F}_i'$, respectively. Finally, we calculate the position of the ith particle at the next time step as follows:

$$\Delta \vec{r}_i = \vec{r}_i(t + \Delta t) - \vec{r}_i^0(t) = \Delta t \sum_j \frac{1}{2} \left(\frac{\partial}{\partial \vec{r}_j^0} D_{ij}^0 + \frac{\partial}{\partial \vec{r}_j'} D_{ij}' \right) + \Delta t \sum_j \frac{1}{2} \left(D_{ij}^0 \vec{F}_j^0 + D_{ij}' \vec{F}_j' \right) / k_B T + \vec{R}_j. \tag{A.9}$$

Here $\vec{R}_j$ obeys the Gaussian distribution where the average value is zero and the variance–covariance is given by the following:

$$\langle R_{i\alpha} R_{j\beta} \rangle = 2\left[\tfrac{1}{2}\left(D^0_{ij} + D'_{ij}\right)\right]\delta_{\alpha\beta}\Delta t. \tag{A.10}$$

References

[1] Bielawski C W, Benitez D and Grubbs R H 2002 *Science* **297** 2041–4
[2] Cho D, Masuoka K, Koguchi K, Asari T, Kawaguchi D, Takano A and Matsushita Y 2005 *Polym. J.* **37** 506–11
[3] Takano A, Kushida Y, Aoki K, Masuoka K, Hayashida K, Cho D, Kawaguchi D and Matsushita Y 2007 *Macromolecules* **40** 679–81
[4] Robertson R M, Laib S and Smith D E 2006 *Proc. Natl Acad. Sci.* **103** 7310–4
[5] Araki S, Nakai T, Hizume K, Takeyasu K and Yoshikawa K 2006 *Chem. Phys. Lett.* **418** 255–9
[6] Calabrese P, Pelissetto A and Vicari E 2002 *J. Chem. Phys.* **116** 8191–7
[7] Orlandini E and Whittington S G 2007 *Rev. Mod. Phys.* **79** 611
[8] Vologodskii A V, Lukashin A V, Frank-Kamenetskii M D and Anshelevich V V 1974 *Sov. Phys.—JETP* **39** 1059–63
[9] Koniaris K and Muthukumar M 1991 *Phys. Rev. Lett.* **66** 2211–4
[10] Quake S R 1974 *Phys. Rev. Lett.* **73** 3317–20
[11] Deguchi T and Tsurusaki K 1997 *Phys. Rev.* E **55** 6245–8
[12] Grosberg A Yu 2000 *Phys. Rev. Lett.* **85** 3858–61
[13] Lai P-K 2002 *Phys. Rev.* E **66** 021805
[14] Shimamura M K and Deguchi T 2002 *Phys. Rev.* E **65** 051802
[15] Dobay A, Dubochet J, Millett K, Sottas P-E and Stasiak A 2003 *Proc. Natl Acad. Sci. USA* **100** 5611–5
[16] Marcone B, Orlandini E, Stella A L and Zonta F 2005 *J. Phys. A: Math. Gen.* **38** L15–21
[17] Orlandini E, Stella A L, Vanderzande C and Zonta F 2007 (*Preprint* 0705.2291)
[18] Rey A, Freire J J and García de la Torre J 1987 *Macromolecules* **20** 342–6
[19] Hernández Cifre J G, Pamies R, López Martinez M C and García de la Torre J 2005 *Polymer* **46** 267–74
[20] Iniesta A and Garcia de la Torre J 1990 *J. Chem. Phys.* **92** 2015–8
[21] Ermak D L and McCammon J A 1978 *J. Chem. Phys.* **69** 1352–60
[22] Ronte J and Prager S 1969 *J. Chem. Phys.* **50** 4831–7
[23] Yamakawa H 1970 *J. Chem. Phys.* **53** 207–46
[24] Burchard W and Schmidt M 1980 *Polymer* **21** 745–9
[25] Zifferer G and Preusser W 2001 *Macromol. Theory Simul.* **10** 397–407
[26] Prentice J J 1982 *J. Chem. Phys.* **76** 1574
[27] Zinn-Justin J 1993 *Quantum Field Theory and Critical Phenomena* (Oxford: Oxford University Press)
[28] Oono Y 1985 *Adv. Chem. Phys.* **61** 301–437
[29] Zimm B H and Stockmayer W H 1949 *J. Chem. Phys.* **17** 1301
[30] Casassa E F 1965 *J. Polym. Sci.* A **3** 605
[31] Oono Y and Kohmoto M 1983 *J. Chem. Phys.* **78** 520
[32] Schaub B and Creamer D B 1987 *Phys. Lett.* A **121** 435–42
[33] Fukatsu M and Kurata J 1966 *J. Chem. Phys.* **44** 4539–45
[34] Duval M, Lutz P and Strazielle C 1985 *Makromol. Chem. Rapid Commun.* **6** 71–6
[35] Hodgson D F and Amis E J 1991 *J. Chem. Phys.* **95** 7653–63
[36] Griffiths P C, Stilbs P, Yu G E and Booth C 1995 *J. Phys. Chem.* **99** 16752–6
[37] Kremer K and Grest G S 1990 *J. Chem. Phys.* **92** 5057–86